Egyptian Journal of Chemistry

http://ejchem.journals.ekb.eg/

Structural Peculiarities of Borate Bioglass Doped With Silver Oxide

Amr M. Abdelghany[1,*], Mahrous S. Meikhail[2], Amin El-Adawy[3], Hosam A. Othman[3] and Eman M. Abdallah[4,*]

[1]*Spectroscopy Department, National Research Center, 33 Elbehouth St., Cairo, 12311, Egypt*
[2]*Physics Department, Faculty of Science, Mansoura University, Mansoura, 35516, Egypt.*
[3]*Physics Department, Faculty of Science, Monofia University, Shebin El-Koom, Egypt.*
[4]*Basic Science Department, Faculty of Physical Therapy, Delta University for Science & Technology, Gamassa, 35712, Egypt.*

Abstract

Modified Hench's bioglass of the basic composition $x$$Ag_2O$(45 B_2O_3, 24.5 CaO, 24.5 Na_2O, 6 P_2O_5) as (x= 0.1, 0.2, 0.4, 0.6, and 0.8 wt.%) were successfully prepared via the melt quenching route. Immersion in phosphate solution (PS) varying times (1→4 weeks) was used to assess the in-vitro behavior of the bulk glassy samples with different silver oxide content. X-ray diffraction XRD, scanning electron microscopy (SEM), and other spectroscopic measurements including Fourier transform infrared (FT-IR) analytical techniques and UV/visible optical measurements before and after prolonged immersion times were used to estimate the bioactive behaviors and to explain the efficiency of bone-bonding. Besides, antimicrobial tests against pathogenic grams were examined and silver ions show varying levels of action against certain bacteria. It was noticed that prolonged immersion periods cause distinct variations that link the vibrational bands as a result of a preferential attack or ion exchange and modifier replacement by silver ions in the glass network causing the hydroxyapatite formation as an indication for bone-bonding ability. Antimicrobial experiments reveal that studied material can be used efficiently as an antibacterial agent

Keywords: Modified Hench bioglass; Hydroxyapatite; Silver ions; Phosphate solution (PS); FTIR; XRD

1. Introduction

Bioactive borate glasses are widely employed in bone implants and tissue engineering processes [1-4]. Many bioactive glasses are used to treat periodontal disease-related bone loss, cystic and surgically-created abnormalities, and conductive deafness, [5-8]. Borate glasses have reduced chemical durability due to their bioactivity. The inclusion of borate in these glasses aids in converging to hydroxyapatite (HA) at a quicker rate. Many bioactive glass researchers have already established that borate is critical for bone development and maintenance, particularly trabecular and alveolar forms [9, 10]. Boron is a potential element that is important for various medicinal processes, including immune function, wound healing, bone formation, and maintenance. Boron is recognized to have an essential part in calcium metabolism, magnesium, and vitamin D and has several vicarious effects on bone. Boron-containing organs and tissues have a diverse distribution, indicating that they play different roles relying on the tissue. Bone and keratinous tissue hold the bulk of the total B content in the human body. As a result, it's plausible to believe that this element is important in hard tissues [9, 11-14]. Consequently, such materials might usher in a new age of bone regeneration biomaterials. Boron has been shown to play a role in angiogenesis and osteogenesis. Bioactive glasses (BGs) that release B ions in a regulated and targeted manner offer a promising treatment option for regenerative medicine of vascularized tissues like bone. The bioactivity and biocompatibility of calcium borate coatings were somewhat reduced when Ag was added.

The inclusion of silver oxide in BGs formulations appears to be a solution to lower the danger of microbiological contamination and the requirement for antibiotic medicine prescriptions by facilitating a localized, continuous, and regulated distribution of silver ions to the implant site during glass breakdown [15]. The borate glass, which contains up to 1 gm wt% Ag, could be used as a coating material for bacterial suppression and improved bioactivity of orthopedic implants like

*Corresponding author e-mail: dr.e_abdallah91@yahoo.com (Eman M. Abdallah)
Receive Date: 31 October 2021, Revise Date: 21 November 2021, Accept Date: 07 December 2021, First Publish Date: 07 December 2021
DOI: 10.21608/EJCHEM.2021.103675.4800

titanium [16]. This might result in a more controlled and slower release of silver, as well as a long-term antibacterial impact from the bioactive glass. A bioactive glass containing up to 1% silver has antibacterial action without toxicity to fibroblasts, indicating that this type of BGs may play a key role in avoiding infection, decreasing pain, and eliminating excessive exudates [17, 18].
Silver's role as an antibacterial agent is well studied in the literature.

The main goal of the presented study is to evaluate the antibacterial effect of silver in modified Hench bioglass and retrace the role of silver ions in the process of bioactivity and in-vitro bonding behavior with time.

2. Materials and Methods

2.1. Sample preparation

The investigation of borate glass, which is made from a precise amount of chemically pure chemicals. For B_2O_3, the ingredients are boric acid (H_3BO_3). Without any additional purification, Sigma Aldrich's modifier oxide (AgO_3) was utilized as supplied. Borate glasses have the formula according to $x$$Ag_2O$(45 B_2O_3, 24.5 CaO, 24.5 Na_2O, 6 P_2O_5) as (x= 0.1, 0.2, 0.4, 0.6, and 0.8 wt.%) added overweight to the batch, whereas Na_2O and CaO have been added in the form of their respective carbonates. In contrast, P_2O_5 was added in the form of ammonium dihydrogen phosphate ($NH_4H_2PO_4$). Under ordinary atmospheric conditions, the weighted batches were combined intoporcelain crucibles and placed in a rising temperature electrical furnace at roughly 1200±10 °C for the appropriate period (60-90 minutes) depending on the glass composition. The crucibles were rotated throughout the melting process to achieve acceptable homogeneity. Table 1 shows the composition of the studied glasses in terms of weight percent.

The melt samples were put into warmed stainless-steel molds of the requisite size, then transported to a muffle furnace set to 450°C. The muffle was kept at this temperature for 1 hour before being turned off to drop to room temperature at a rate of roughly 30 degrees per hour. To prevent the sample from breaking as a result of residual stress. The grain approach was used to make the bioactive glass, which various scientists have used.

To avoid thermal shocks, the annealed samples were placed on the furnace door for 5 minutes. The glassy samples were then placed straight into the furnace and kept at the heat treatment temperature for the necessary amount of time before cooling to room temperature. As a result, each glass was gently heated to 450 °C for 5 hours to produce adequate nuclei sites and then heated to the second specified crystal growth temperature of 650 °C. After a 6-hour holding period, the specimens were allowed to drop to ambient temperature at a rate of 20 °C/hour within the muffle.
For one week, two weeks, three weeks, and four weeks, glass grains were submerged in a 0.25-mole disodium hydrogen phosphate (Na_2HPO_4) solution.

During the immersion period, the solution was changed every two days in all cases.

Table (1) Sample nomination and composition

Glass No.	*Composition [wt.%]*				
	Na_2O	***CaO***	***B_2O_3***	***P_2O_5***	Ag_2O
GAg0	24.5	24.5	45	6	0
GAg1	24.5	24.5	45	6	0.1
GAg2	24.5	24.5	45	6	0.2
GAg3	24.5	24.5	45	6	0.4
GAg4	24.5	24.5	45	6	0.6
GAg5	24.5	24.5	45	6	0.8

2.2. Measurements Techniques

Using the KBr disc technique, the investigated glasses' infrared spectra were recorded by a Nicolet iS10 (USA) FTIR spectrometer at room temperature. Spectra were obtained in the wavenumber range between 4000 and 400 cm^{-1} with a resolution of 2 cm^{-1}. For each sample, there are two recorded spectra. After controlled crystallization and immersion operations, the XRD method was used to detect crystalline phases existent or generated within the samples and retrace constitutional changes. XRD patterns were carried out using a Philips PW1390 x-ray diffractometer to measure the glass-ceramic samples in the form of finely ground powder. A source of CuKα radiation (λCuKα = 0.15406 nm) has been utilized. Microstructure observations of glass-ceramic samples were made using a scanning electron microscope. SEM studies of samples were made with aJEOL JSM-6510LV, USA which is attached to an EDAX unit and a 20 kV accelerating voltage. To decrease the charging influence of the electron beam, the surfaces of all samples were vacuum evaporated with a 3.5 nm thin layer of Au. The antibacterial activity of the produced compounds was tested against a 2 gram-positive bacteria panel (*Bacillus subtilis, Staphylococcus aureus*). In addition, there are 2 Gram-negative bacteria (*Pseudomonas aeuroginosa, Escherichia coli*). Two fungi were used to assess the compounds' antifungal properties (*Candida albicans, Aspergillus flavus*). The formula used to calculate the complex's percent activity index was as follows:[14, 15]

$$\%\ \boldsymbol{Activity\ Index} = \frac{\boldsymbol{Zone\ of\ inhibition\ by\ test\ compound\ (diametre)}}{\boldsymbol{Zone\ of\ inhibition\ by\ standard\ (diametre)}}\mathbf{X100}$$

Results

2.3. FTIR spectra before and after immersion

Fourier transform infrared spectroscopy is a valuable and powerful technique used to study and retrace structural and compositional changes. The primary spectral bands found in their spectra may be ascribed as shown in **Fig. (1)** and ascribed to such distinct structural groups as mentioned in **Table (2)**. Borate glasses are generally composed of two structural forming groups (BO_3, BO_4).

The measured FTIR spectrum was analyzed and deconvoluted using the peak fit 4.12 program via two stages regime [19, 20]. Stage one involves estimation of the minimum number and position of spectral bands corresponding to different vibrational modes expected to be present in the structure, including resolved maxima and well-settled shoulders and kinks, while the second stage involves adding weakercertified asymmetric modes previously published for the same composition. Iterative calculations were done until the coefficient of determination (r^2) reached an acceptable value [21].

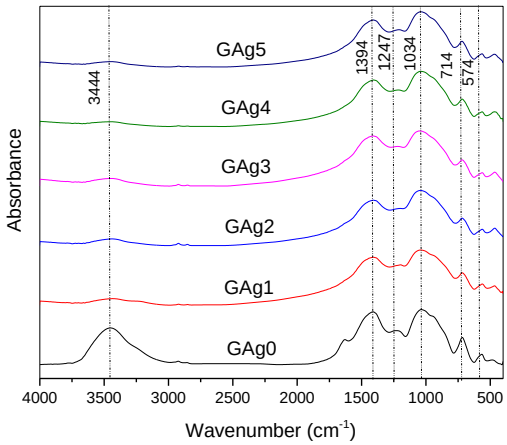

Fig. 1. FTIR absorption spectra silver oxide doped with borate bioglasses before immersion in phosphate solution.

Table (2): Infrared absorption bands observed in the borate glasses and their assignment [20-24]

Peak position [cm^{-1}]	Assignment
456	Vibrations of metal cations
558	bending vibrations of O-P-O units
724	BO3–O–BO4 bond-bending vibrations
877	Diborate groups
1036	Penta borate group
1215	Tri-, Penta-, tetraborate boroxal groups
1406	Presence of pyroborate, orthoborate groups containing BO3

Fig. (2) Shows an exemplified deconvoluted data of glass containing Ag ions before immersion in phosphate solution. Band position, FWHM, and area

obtained from such deconvolution for all samples can be summarized as shown in **Table (3).**

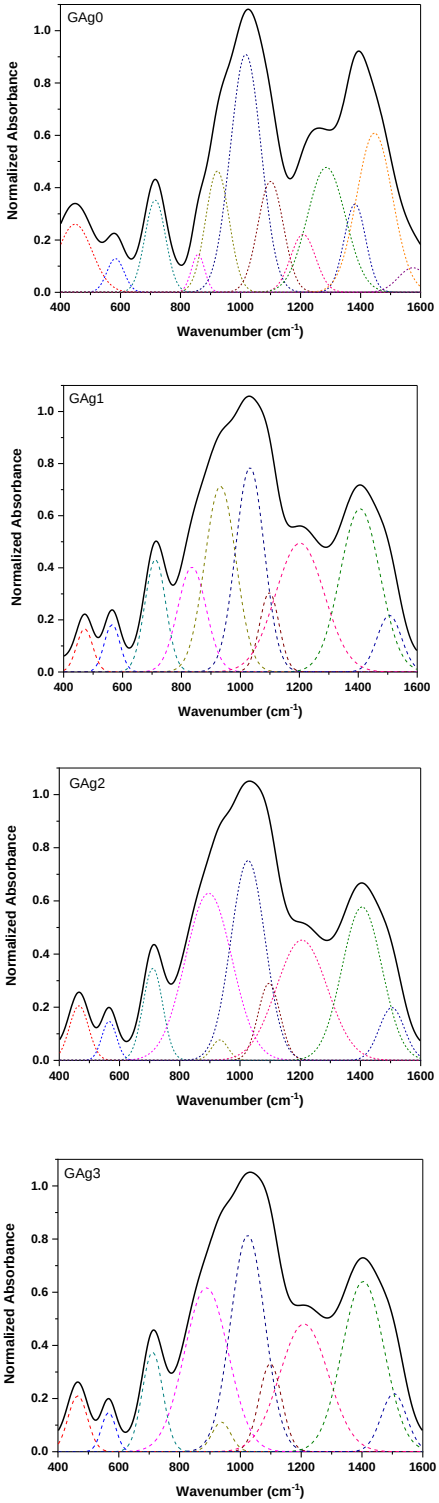

Fig. (2) deconvoluted data of glass containing Ag ions before immersion in the phosphate solution

Table (3): Band position, FWHM, and area obtained from such deconvolution for all samples of silver oxide dopant with borate glasses before immersion in a phosphate solution

Sample	Peak	1	2	3	4	5	6	7	8
GAg0	**Position**	715	858	920	1025	1110	1211	1267	1399
	Area	32	7	37	153	16	34	14	151
	F.W.H.M	81	50	90	145	79	91	71	184
GAg1	**Position**	711	835	932	1032	1098	1202	1406	1505
	Area	38	48	94	95	25	102	105	22
	F.W.H.M	84	113	124	114	77	194	158	96
GAg2	**Position**	710	896	933	1026	1096	1205	1405	1504
	Area	28	122	5	107	26	95	95	20
	F.W.H.M	77	182	64	134	85	198	156	98
GAg3	**Position**	710	896	933	1026	1096	1205	1405	1504
	Area	28	122	5	107	26	95	95	20
	F.W.H.M	79	169	72	132	87	188	162	98
GAg4	**Position**	712	877	934	1018	1095	1210	1402	1504
	Area	34	91	12	127	32	83	108	21
	F.W.H.M	84	148	73	134	87	173	161	98
GAg5	**Position**	714	876	933	1018	1094	1209	1405	1505
	Area	31	88	14	126	29	90	102	21
	F.W.H.M	79	146	74	132	84	177	154	97

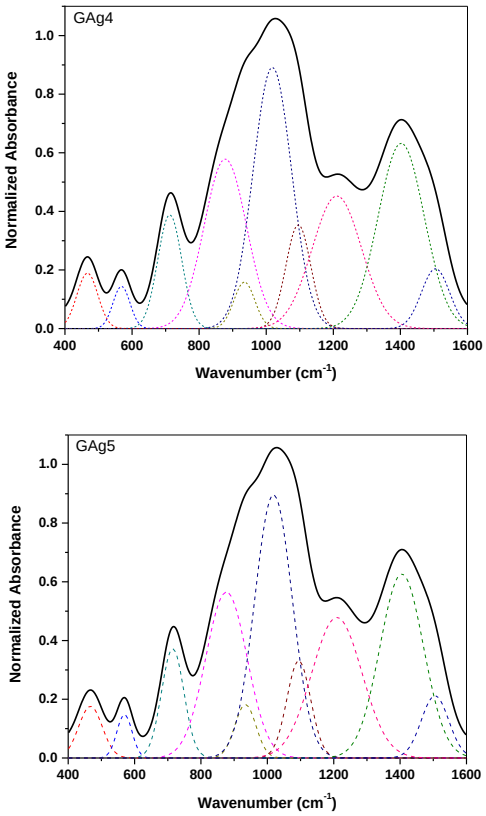

Fig. 2. Deconvoluted FT-IR spectra of modified borate glass containing silver oxide samples before immersion in a phosphate solution

The fraction N4 of borate glasses was calculated before immersion in phosphate solution as shown in **Fig. (3)** and listed in **Table (4)** adopting the relative area of both (BO_3) and (BO_4) units in the respective analyzed peaks using the following formula [20, 25]:

$$\mathbf{N4} = \frac{\mathbf{BO4}}{\mathbf{BO3} + \mathbf{BO4}}$$

A new spectral band is identified at about 1234 cm^{-1} and1226 cm^{-1}. This can be assumed to be due to the formation of bridging bonds of Ag—BO_3[20-24], which may affect its transformation to BO_4, or it may enter as a modifier which in such a case raises the total modifier content, which in turnAgBO would be formed. Another dominant shift in the low-frequency band at (600-800) towards a higher wavenumber can be simply seen. Subsequent additions of $AgNO_3$ (0-0.8Wt %) have the same effect on the structure of glasses. The biggest shift of the peaks at 916–876 cm^{-1} is observed in samples which indicates that when the content of $AgNO_3$ increases, the content of asymmetric BO_3 (borate tetrahedral containing AgBO) becomes dominant in the glass network structure.It can be presumed that the increasing polarization of silver ions with the increased content of their contributes to the formation of Ag^+ modified boron– oxygen rings and their chains.

Table (4) the fraction N4 calculated from FTIR data

Ag Conc.	N_4
0	٠,٤٧٨٨٥
0.1	٠,٤٩٤٥٤
0.2	٠,٥٢٠٣٦
0.4	٠,٥٢٠٣٦
0.6	٠,٥١٥٩٤
0.8	٠,٥١٢١٨

The absorptions of Ag ions at 456 cm^{-1} show that it is of the good network former of glasses in this region [26, 27].From all considerations which are based on the correlation between structural changes assessed by FTIR, it is confirmed that the phenomenon of boron back conversion is the main reason for

changing the borate network upon the addition of $AgNO_3$. The observed $BO_3 \leftrightarrow BO_4$ conversion strongly depends on not only the relative modifier B_2O_3 ratios but also the Ag ions content in the glass.

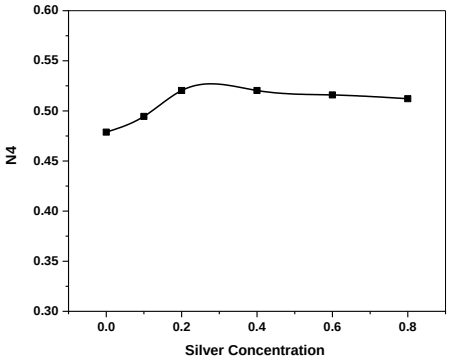

Fig. (3). Variation of N_4 fraction of glass containing silver oxide dopant with Borate glasses before immersion in phosphate solution.

FTIR spectral data were recorded after immersion in phosphate solution for different time intervals, from one to four weeks. Obtained data were analyzed and compared with that for the same samples before immersion. Base glass (GAg0) and glass containing 0.4 Ag (GAg3) are shown as an example in **Figure (4. a, b)**. In all samples, the fair comparison shows the appearance of characteristics peaks at 1636 cm^{-1}, 560 cm^{-1}, and 610 cm^{-1} that indicating the formation of hydroxyapatite (HA) after different times of immersion in phosphate solution [18].

Deconvolution analysis technique in combination with experimental FTIR data was employed to calculate the fractions of four coordinated borons N4 after immersion in phosphate solution for different time intervals. Obtained data were summarized as shown in **Table 5**. It was noted that the addition of silverions results in a gradual decrease of N_4 during the immersion process over the four weeks and combined with the increase of silver concentration up to 0.8 Wt%. It was also noted that there is a gradual increase of BO3 group decomposition during the immersion process and also combined with the increase of silver concentration up to 0.8 Wt%.

Table (5) Calculated the fractions of four coordinated borons N4 after immersion in phosphate solution for different time intervals

Ag Content	N4			
	1Week	2Weeks	3Weeks	4Weeks
0.0	0.414	0.454	0.513	0.497
0.1	0.481	0.483	0.408	0.521
0.4	0.455	0.514	0.503	0.586
0.6	0.503	0.463	0.419	0.546
0.8	0.543	0.455	0.408	0.518

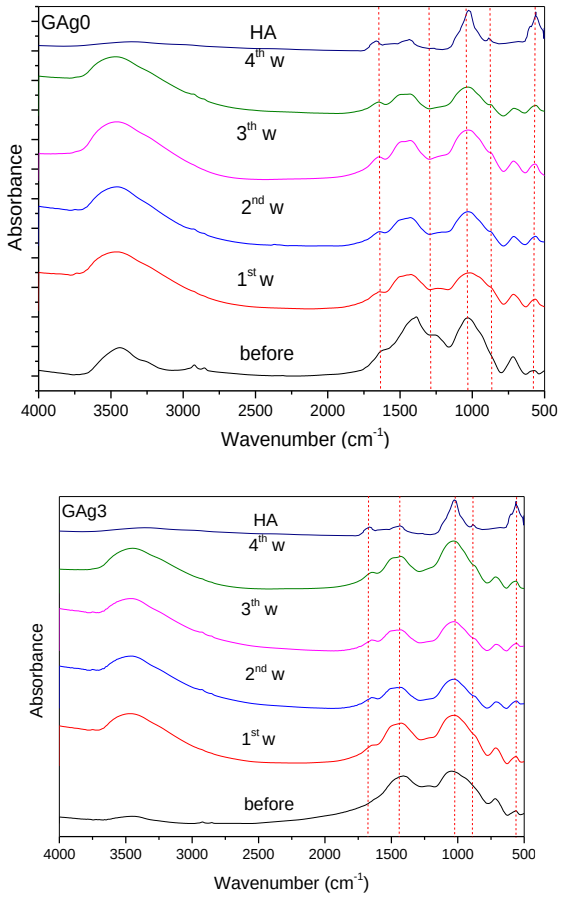

Fig. 4. Exemplified FTIR spectral data before and after different immersion times in phosphate solution

2.4. X-ray diffraction patterns of glass samples before and after varying immersion periods.

Recently,much research has been devoted to the development of new classes of materials suitable for specific purposes in the field of medicine materials that are used to stimulate biochemical responses of living tissues to achieve chemical bonding combined with biological fixation between tissues and prosthesis are of interest. Many bioactive and biocompatible glasses have been developed during the last decades, and their bone-bonding abilities have also been studied both in vitro and in vivo. The property that can be evaluated both in qualitative and quantitative regimes was the formation of hydroxylapatite (HA) layer on materials surfaces, upon immersion in the relevant physiological solutions. The mechanism of interaction, bonding, and bone formation has been extensively studied and interpreted [28-31]. It was considered that borate bioglass follows a contracting volume regime, where the HA layer is formed originally at the surface of the material and then

reacts radially inward to the content of the material until it completely reacted. Different techniques were employed to investigate and retrace this phenomenon. Borate glasses represent a vital and widespread type of glass that consists mainly of borate units that have an important character that results from their ability to be formed in two different structural groups, namely (BO_3) and (BO_4) units that govern the physical and chemical characteristics of studied samples. The arrangement of such structural units indicates the uses and applications that they can be involved in.

Generally, glass is defined as an amorphous or non-periodic material that results from a fusion process whose properties depend mainly on the nominal composition and method of preparation. **Fig. (5)** reveals X-ray diffraction of the studied borate glasses of composition like that of Hench Bioglass with full replacement of silica (SiO_2) by equivalent boron oxide (B_2O_3) (45 B_2O_3, 24.5 CaO, 24.5 Na_2O, 6 P_2O_5) as a parent glass with additional samples containing different concentrations of dopant silver oxide (0.1, 0.2, 0.4, 0.6 and 0.8Wt%). The diffraction patterns show the amorphous nature of prepared samples even withincreasing content of silver ions up to 0.8 Wt %.

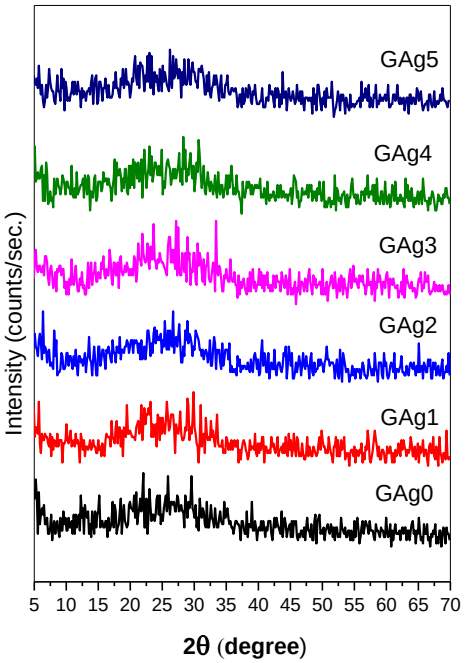

Fig. (5). XRD spectra of samples of silver oxide doped borate bioglasses before immersion in phosphate solution.

Fig. (6) illustrates the X-ray diffraction data of the samples of silver oxide doped borate bioglasses after increasing immersion in phosphate solution from 1, 2, and 3 –4 weeks.

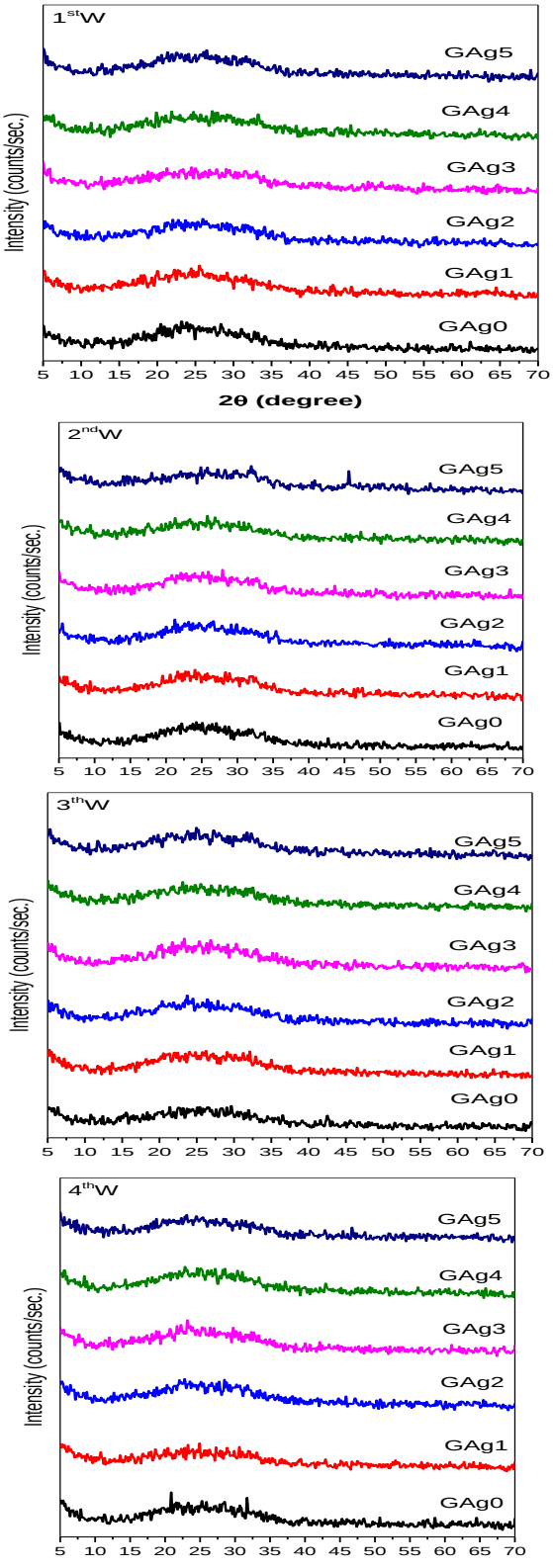

Fig. (6.a). XRD spectra of samples of silver oxide doped borate bioglasses after immersion in phosphate solution for different time intervals.

The data shows the following variations:

(i) The base sample (GAg0) immersed for 1, 2, 3 and 4 weeks in phosphate solution shows three identified crystalline phases, namely: (i) a main crystalline phase of hydroxyapatite. (ii) the second phase of calcium phosphate (iii) the third phase of calcium borate.

(ii) The samples start from adding silver (GAg1) to concentration (GAg5) immersed for 1, 2, 3, and 4 weeks in phosphate solution show four identified crystalline phases but with a different ratio, (i) A main crystalline phase of hydroxyapatite. (ii) the second phase of calcium phosphate ($Ca(PO_3)_2$). (iii) The third phase of calcium borate (CaB_4O_7) [32]. (iv)The fourth phase of silver phosphate ($AgPO_3$) [33].

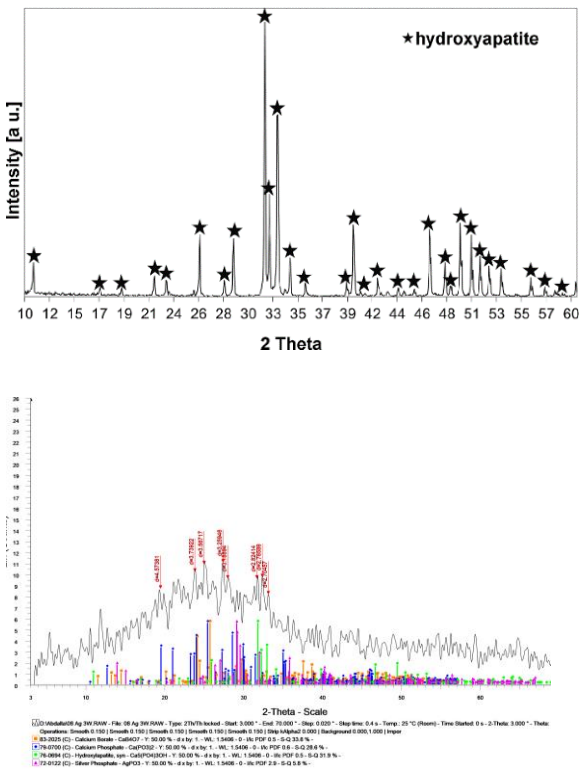

Fig. (6.b). XRD vierge data 0fGAg5 after 2W and literature XRD spectra card of pure HA card no.76-0694(C)-Hydroxylapatite [34].

2.5. Scanning electron microscopic investigations data

SEM micrographs of the synthesized samples before and after a prolonged time of immersion (4weeks) in phosphate solution were recorded to estimate the morphological variations related to the structural variations. All samples before immersion reveal the same texture related to the amorphous nature justified by XRD results. While after (4weeks) immersion reveals both needle-like and cotton-like structures of the crystalline forms interpreted using XRD data [35].

The EDAX data of the samples GAg3 and GAg5 reveal nearly the same results, indicating the formation of a homogenous surface layer of HA with a calcium to phosphate ratio ranging between 1.6 to about 1.7 which agrees with the date reported for HA [35]. EDAX results justify the presence of specific peaks at energies of 3.69, 0.3413, 1.051, 2.013, 0.183, and 0524 keV related to Ca Kα, Ca Lα, Na Kα, P Kα, B Kα, and O Kα respectively. Figure (7. a, b) reveals EDAX analysis and SEM micrographs of the base glassy sample before and after 4 weeks immersion in PS.

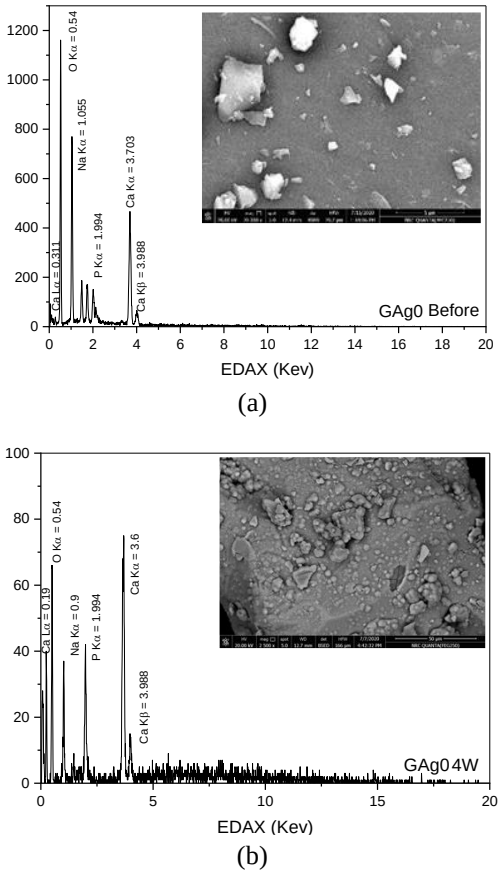

Fig. (7. a, b) EDAX analysis and SEM micrographs of the base glassy sample before and after 4 weeks immersion in PS.

Samples that contain different amounts of silver oxide as shown in Figures (8. a:d) reveal the appearance of extra peaks at 0.06, 2.67, and 3.15 keV attributed to Mα, Lβ, and Lαof silver presented within the matrix in oxide form (where Mα is the energy emitted from the atom when electron transferred from the first excited state of M level, Lβ and Lα is the energy emitted from the atom when

electron transferred from both second and first excited state of L level respectively). The sample GAg3 at different immersion times is given as an example describing the role of silver and immersion times in the formation of HA.

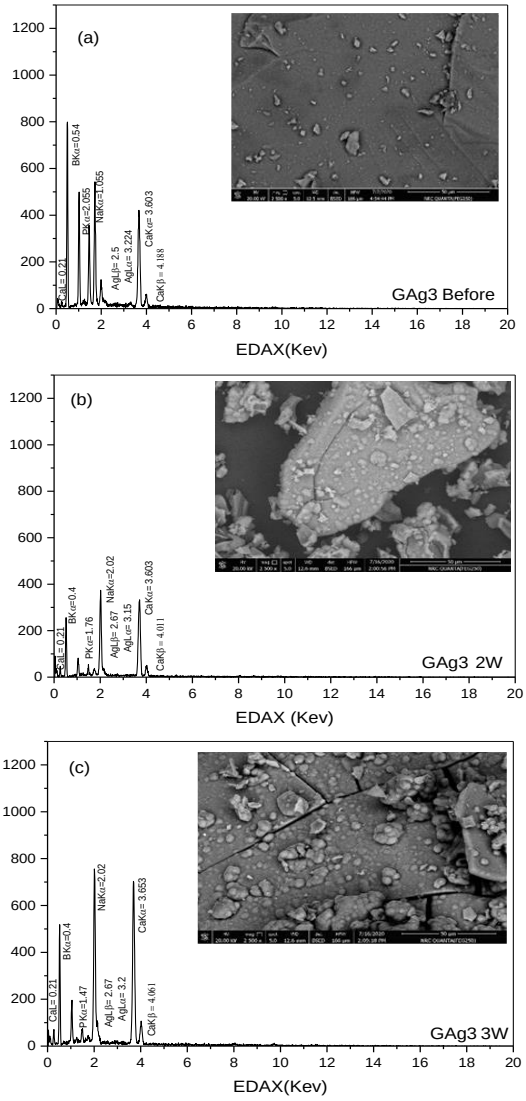

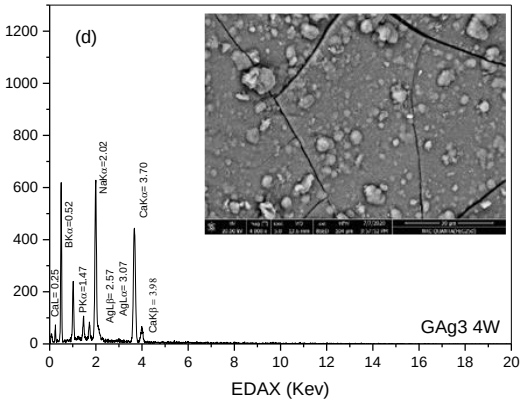

Fig. (8. a:d) EDAX analysis and SEM micrographs of glassy sample GAg3 before and after different times of immersion in PS.

2.6. Antimicrobial testof silver oxide doped borate bioglasses.

The antibacterial activity of a common standard antibiotic ampicillin and antifungal Colitrimazole was also recorded using the same procedure, at the same concentration and solvents. The obtained data shows the activity of silver ions against different types of microbes as listed in **Table (6)**.

The variation in the zone of inhibition diameters might be linked to differences in nanoparticle mobility in cells due to size differences creating varying amounts of reactive oxygen species (ROS).

Table (6): Antimicrobial dataof silver oxide doping borate bioglasses.

Glass	*E. coli* (mg/ml)		*Pseudomonas aeuroginosa* (mg/ml)		*S. aureus* (mg/ml)		*Bacillus subtilis* (mg/ml)		*C. Albicans* (mg/ml)		*A. flavus* (mg/ml)	
	D	**A**	**D**	**A**	**D**	**A**	**D**	**A**	**D**	**A**	**D**	**A**
GAg0	5	20	10	43.5	13	54.2	12	52.2	12	44.4	16	64
GAg1	10	40	16	69.6	19	79.2	17	73.9	15	55.5	18	72
GAg2	NA	----	2	8.7	3	12.5	5	21.7	4	14.8	7	28
GAg3	7	28	13	56.5	10	41.7	15	65.2	11	40.7	16	64
GAg4	NA	----	NA	----	NA	----	2	8.7	2	8	4	16
GAg5	NA	----	2	8.7	NA	----	3	13	NA	----	2	8
Ampicillin	25	100	23	100	24	100	23	100	NA	----	NA	----
Colitrimazole	NA	----	NA	----	NA	----	NA	----	27	100	25	100

D Diameter of inhibition zone (mm), A Activity index%

Conclusion

The bioactive glass system with variable concentrations of Ag_2O is synthesized to probe the influence of silver ions on structure and bioactivity. The in vitro bioactivity of these glasses is studied by immersing them in phosphate solution over different periods (1-4 weeks). The formation of the crystalline HA layer on the surface of all the specimens was examined by XRD, FTIR SEM, EDAX, and anti-microbial studies. The quantitative analyses of these results have indicated that all the glasses are proved to be bioactive and the silver ions which occupy modifying positions facilitate more degradation and bioactivity. It was found from these studies thato.4 Wt% and 0.8Wt% of silver oxide (GAg3) and (GAg5) samples are the optimum concentrations in terms of the percentage of hydroxyapatite (HA) layer formation and compatibility with the body, with the availability of antimicrobial properties due to silver ions.

It has also been shown that the optimal soaking periods to obtain the best-desired results are three weeks with a concentration 0.4Wt% silver oxide (GAg3) sample and four weeks with concentration 0.8Wt% silver oxide (GAg5) sample as the soaking period more than that may cause the beginning of the decomposition of the material according to the obtained results from EDAX.

Finally, it can be concluded that the presence of Ag_2O yields better bioactivity and less toxicity than others.

Conflicts of interest

The authors declare that there is no conflict of interest

Formatting of funding sources

Authors receive no funding

References

1. Rahaman, M. N., Day, D. E., Bal, B. S., Fu, Q.`, Jung, S. B., Bonewald, L. F., & Tomsia, A. P. (2011). Bioactive glass in tissue engineering. *Actabiomaterialia*, *7*(6), 2355-2373 doi.org/10.1016/j.actbio.2011.03.016 .
2. Kaur, G., Pandey, O. P., Singh, K., Homa, D., Scott, B., & Pickrell, G. (2014). A review of bioactive glasses: their structure, properties, fabrication and apatite formation. *Journal of Biomedical Materials Research Part A: An Official Journal of The Society for Biomaterials, The Japanese Society for Biomaterials, and The Australian Society for Biomaterials and the Korean Society for Biomaterials*, *102*(1), 254-274 doi.org/10.1002/jbm.a.34690.
3. Kargozar, S., Baino, F., Hamzehlou, S., Hill, R. G., & Mozafari, M. (2018). Bioactive glasses: sprouting angiogenesis in tissue engineering. *Trends in biotechnology*, *36*(4), 430-444 doi.org/10.1016/j.tibtech.2017.12.003.
4. Abdelghany, A. M., Ouis, M. A., Azooz, M. A., ElBatal, H. A., & El-Bassyouni, G. T. (2016). Role of SrO on the bioactivity behavior of some ternary borate glasses and their glass ceramic derivatives. *Spectrochimica Acta Part A: Molecular and Biomolecular Spectroscopy*, *152*, 126-133doi.org/10.1016/j.tibtech.2017.12.003 .
5. Gillam, D. G., Tang, J. Y., Mordan, N. J., & Newman, H. N. (2002). The effects of a novel Bioglass® dentifrice on dentine sensitivity: a scanning electron microscopy investigation. *Journal of Oral Rehabilitation*, *29*(4), 305-313 doi.org/10.1046/j.1365-2842.2002. 00824.x.
6. Lee, B. S., Tsai, H. Y., Tsai, Y. L., Lan, W. H., & Lin, C. P. (2005). In vitro study of DP-bioglass paste for treatment of dentin hypersensitivity. *Dental materials journal*, *24*(4), 562-569 doi.org/10.4012/dmj.24.562.
7. Erol-Taygun, M., Zheng, K., & Boccaccini, A. R. (2013). Nanoscale bioactive glasses in medical applications. *International Journal of Applied Glass Science*, *4*(2), 136-148.doi.org/10.1111/ijag.12029
8. Abbasi, Z., Bahrololoom, M. E., Shariat, M. H., & Bagheri, R. A. F. A. T. (2015). Bioactive glasses in dentistry: a review. *Journal of Dental Biomaterials*, *2*(1), 1-9 doi.org/10.1111/ijag.12029.
9. Gallardo-Williams, M. T., Maronpot, R. R., Turner, C. H., Johnson, C. S., Harris, M. W., Jayo, M. J., & Chapin, R. E. (2003). Effects of boric acid supplementation on bone histomorphometry, metabolism, and biomechanical properties in aged female F-344 rats. *Biological trace element research*, *93*(1), 155-169 doi.org/10.1385/BTER:93:1-3:155.
10. Nielsen, F. H., & Meacham, S. L. (2011). Growing evidence for human health benefits of boron. *Journal of Evidence-Based Complementary & Alternative Medicine*, *16*(3), 169-180 doi.org/10.1177/2156587211407638.
11. Lakhkar, N. J., Lee, I. H., Kim, H. W., Salih, V., Wall, I. B., & Knowles, J. C. (2013). Bone formation controlled by biologically relevant inorganic ions: role and controlled delivery from phosphate-based glasses. *Advanced drug delivery reviews*, *65*(4), 405-420 doi.org/10.1016/j.addr.2012.05.015.

12. Zamet, J. S., Darbar, U. R., Griffiths, G. S., Bulman, J. S., Brägger, U., Bürgin, W., & Newman, H. N. (1997). Particulate bioglass® as a grafting material in the treatment of periodontal intrabony defects. *Journal of clinical periodontology*, *24*(6), 410-418 doi.org/10.1111/j.1600-051X.1997.tb00205.x.
13. Moseman, R. F. (1994). Chemical disposition of boron in animals and humans. *Environmental health perspectives*, *102*(suppl 7), 113-117 doi.org/10.1289/ehp.94102s7113.
14. Nielsen, F. H. (2000). The emergence of boron as nutritionally important throughout the life cycle. *Nutrition*, *16*(7-8), 512-514 DOI: 10.1016/s0899-9007(00)00324-5 .
15. El-Kady, A. M., Ali, A. F., Rizk, R. A., & Ahmed, M. M. (2012). Synthesis, characterization and microbiological response of silver doped bioactive glass nanoparticles. *Ceramics International*, *38*(1), 177-188 doi.org/10.1016/j.ceramint.2011.05.158.
16. Luo, S. H., Xiao, W., Wei, X. J., Jia, W. T., Zhang, C. Q., Huang, W. H., ... & Day, D. E. (2010). In vitro evaluation of cytotoxicity of silver-containing borate bioactive glass. *Journal of Biomedical Materials Research Part B: Applied Biomaterials*, *95*(2), 441-448 doi.org/10.1002/jbm.b.31735.
17. Durand, L. A. H., Vargas, G. E., Romero, N. M., Vera-Mesones, R., Porto-López, J. M., Boccaccini, A. R., ... & Gorustovich, A. (2015). Angiogenic effects of ionic dissolution products released from a boron-doped 45S5 bioactive glass. *Journal of Materials Chemistry B*, *3*(6), 1142-1148 DOI: 10.1039/C4TB01840K.
18. Abo-Naf, S. M., Khalil, E. S. M., El-Sayed, E. S. M., Zayed, H. A., & Youness, R. A. (2015). In vitro bioactivity evaluation, mechanical properties and microstructural characterization of Na_2O–CaO–B_2O_3–P_2O_5 glasses. *Spectrochimica Acta Part A: Molecular and Biomolecular Spectroscopy*, *144*, 88-98 doi.org/10.1016/j.saa.2015.02.076.
19. Abdelghany, A. M. (2010). The elusory role of low level doping transition metals in lead silicate glasses. *Silicon*, *2*(3), 179-184 doi.org/10.1007/s12633-010-9053-8.
20. Kamitsos, E. I. (2003). Infrared studies of borate glasses. *Physics and Chemistry of Glasses*, *44*(2), 79-87.
21. Abdelghany, A. M. (2013). Novel method for early investigation of bioactivity in different borate bio-glasses. *Spectrochimica Acta Part A: Molecular and Biomolecular Spectroscopy*, *100*, 120-126 doi.org/10.1016/j.saa.2012.02.051.
22. Abdelghany, A. M., ElBatal, H. A., & EzzElDin, F. M. (2012). Bone bonding ability behavior of some ternary borate glasses by immersion in sodium phosphate solution. *Ceramics International*, *38*(2), 1105-1113doi.org/10.1016/j.ceramint.2011.08.038.
23. Gautam, C., Yadav, A. K., & Singh, A. K. (2012). A review on infrared spectroscopy of borate glasses with effects of different additives. *International Scholarly Research Notices*, *2012***doi.org/10.5402/2012/428497.**
24. Winterstein-Beckmann, A., Möncke, D., Palles, D., Kamitsos, E. I., & Wondraczek, L. (2013). Structure–property correlations in highly modified Sr, Mn-borate glasses. *Journal of non-crystalline solids*, *376*, 165-174 DOI:10.1016/j.jnoncrysol.2013.05.029.
25. Yiannopoulos, Y. D., Chryssikos, G. D., & Kamitsos, E. I. (2001). Structure and properties of alkaline earth borate glasses. *Physics and chemistry of glasses*, *42*(3), 164-172.
26. Menazea, A. A., & Abdelghany, A. M. (2020). Precipitation of silver nanoparticle within silicate glassy matrix via Nd: YAG laser for biomedical applications. *Radiation Physics and Chemistry*, *174*, 108958 doi.org/10.1016/j.radphyschem.2020.108958.
27. Delben, J., Pimentel, O., Coelho, M., Candelorio, P., Furini, L., Alencar dos Santos, F., ... & Delben, A. (2009). Synthesis and thermal properties of nanoparticles of bioactive glasses containing silver. *Journal of thermal analysis and calorimetry*, *97*(2), 433-436 doi.org/10.1007/s10973-009-0086-4.
28. Vitale-Brovarone, C., Verné, E., Robiglio, L., Martinasso, G., Canuto, R. A., & Muzio, G. (2008). Biocompatible glass–ceramic materials for bone substitution. *Journal of Materials Science: Materials in Medicine*, *19*(1), 471-478 DOI: 10.1007/s10856-006-0111-0.
29. Huang, W., Day, D. E., Kittiratanapiboon, K., & Rahaman, M. N. (2006). Kinetics and mechanisms of the conversion of silicate (45S5), borate, and borosilicate glasses to hydroxyapatite in dilute phosphate solutions. *Journal of Materials Science: Materials in Medicine*, *17*(7), 583-**596**DOI: 10.1007/s10856-006-9220-z.
30. Cole, K. A., Funk, G. A., Rahaman, M. N., & McIff, T. E. (2020). Characterization of the conversion of bone cement and borate bioactive glass composites. *Journal of Biomedical Materials Research Part B: Applied Biomaterials*, *108*(4), 1580-1591 doi.org/10.1002/jbm.b.34505.
31. Islam, M. T., Macri-Pellizzeri, L., Sottile, V., & Ahmed, I. (2021). Rapid conversion of highly porous borate glass microspheres into hydroxyapatite. *Biomaterials Science*, *9*(5), 1826-1844 DOI: 10.1039/D0BM01776K.
32. Mutlu, S. I., Simsek, U. G., Iflazoglu, S., Yilmaz, A., Mutlu, M., & Seven, P. T. (2021). Impact of dietary calcium tetraborate supplementation on the mineral content of egg and eggshell of laying quails. *GSC Biological and Pharmaceutical*

Sciences, *15*(1), 018-026 doi.org/10.30574/gscbps.2021.15.1.0090**.**

33. Benyounoussy, S., Bih, L., & El Bouari, A. (2020). Structure and dielectric properties in silver phosphate $AgPO_3$ glass–ceramic. *Materials Today: Proceedings*, *30*, 933-936 doi.org/10.1016/j.matpr.2020.04.353**.**
34. Tyliszczak, B., et al. "Stabilization of ceramics particles with anionic polymeric dispersants." Journal of nanoscience and nanotechnology 12.12 (2012): 9312-9318.doi.org/10.1166/jnn.2012.6763
35. Samadian, H., Mobasheri, H., Azami, M., & Faridi-Majidi, R. (2020). Osteoconductive and electroactive carbon nanofibers/hydroxyapatite nanocomposite tailored for bone tissue engineering: in vitro and in vivo studies. *Scientific Reports*, *10*(1), 1-**14** doi.org/10.1038/s41598-020-71455-3**.**